Massive accumulation of luminal protease-deficient axonal lysosomes at Alzheimer's disease amyloid plaques

Swetha Gowrishankar[a,b,c], Peng Yuan[b,d], Yumei Wu[a,b,c], Matthew Schrag[d], Summer Paradise[a,b,c], Jaime Grutzendler[b,d], Pietro De Camilli[a,b,c,1], and Shawn M. Ferguson[a,b,1]

[a]Department of Cell Biology, [b]Program in Cellular Neuroscience, Neurodegeneration and Repair, [c]Howard Hughes Medical Institute, and [d]Department of Neurology, Yale University School of Medicine, New Haven, CT 06510

Contributed by Pietro De Camilli, May 26, 2015 (sent for review April 29, 2015; reviewed by Thomas Biederer and Joachim Herz)

Through a comprehensive analysis of organellar markers in mouse models of Alzheimer's disease, we document a massive accumulation of lysosome-like organelles at amyloid plaques and establish that the majority of these organelles reside within swollen axons that contact the amyloid deposits. This close spatial relationship between axonal lysosome accumulation and extracellular amyloid aggregates was observed from the earliest stages of β-amyloid deposition. Notably, we discovered that lysosomes that accumulate in such axons are lacking in multiple soluble luminal proteases and thus are predicted to be unable to efficiently degrade proteinaceous cargos. Of relevance to Alzheimer's disease, β-secretase (BACE1), the protein that initiates amyloidogenic processing of the amyloid precursor protein and which is a substrate for these proteases, builds up at these sites. Furthermore, through a comparison between the axonal lysosome accumulations at amyloid plaques and neuronal lysosomes of the wild-type brain, we identified a similar, naturally occurring population of lysosome-like organelles in neuronal processes that is also defined by its low luminal protease content. In conjunction with emerging evidence that the lysosomal maturation of endosomes and autophagosomes is coupled to their retrograde transport, our results suggest that extracellular β-amyloid deposits cause a local impairment in the retrograde axonal transport of lysosome precursors, leading to their accumulation and a blockade in their further maturation. This study both advances understanding of Alzheimer's disease brain pathology and provides new insights into the subcellular organization of neuronal lysosomes that may have broader relevance to other neurodegenerative diseases with a lysosomal component to their pathology.

lysosome | Alzheimer's | progranulin | axonal transport | cathepsin

Alzheimer's disease (AD) is the most common form of dementia associated with aging. Nonetheless, more than a century after the original definition of the disease, the identification of the fundamental cell biological processes that cause AD remains a major challenge. Major defining features of AD brain pathology, as elucidated by molecular and genetic studies in humans and mice, are as follows: the proteolytic processing of the amyloid precursor protein (APP) by the successive action of β- and γ-secretases to generate the toxic Aβ peptides, the accumulation of extracellular aggregates of Aβ, synapse dysfunction, and death of specific subpopulations of neurons (1–6). However, although mutations that result in enhanced APP expression and/or altered processing of APP into Aβ peptides drive the development of a subset of early onset familial forms of AD, the causes of the vastly more common late-onset AD are much less well understood.

One major aspect of AD pathology that is observed in both humans and mouse models of the disease is the formation of amyloid plaques. These structures contain a core of aggregated extracellular Aβ that is surrounded by swollen, dystrophic neurites and microglial processes (7–13). Multiple studies in humans and mice have additionally reported an elevated abundance of putative lysosomes and/or lysosomal proteins around amyloid plaques (9–11, 14–16). These observations indicate an influence of extracellular β-amyloid deposits on the physiology of surrounding cells and raise questions about the underlying cell biological mechanisms and the contributions of such pathological changes to AD.

The goal of this study was to investigate the cell biology of AD amyloid plaques to advance understanding of how the interactions between extracellular Aβ aggregates and surrounding brain tissues might contribute to disease pathology. Through studies of mouse models of AD, we found a robust relationship between extracellular Aβ aggregates and the massive accumulation of lysosomes (but not other organelles) within swollen axons adjacent to such aggregates. A striking new feature of the lysosomes that accumulate within these dystrophic axons is their relatively low levels of multiple lysosomal proteases. Because we also identified a subpopulation of lysosomes with similar properties in the distal neuronal compartments of normal brain tissue and primary neuron cultures, the distinct composition of the axonal lysosomes that accumulate at amyloid plaques most likely reflects a blockade in their retrograde transport and maturation. More broadly, our characterization of a distinct population of axonal lysosomes that is selectively accumulated at amyloid plaques provides a foundation for the future elucidation of the mechanisms that underlie their biogenesis, function, and contributions to neuronal physiology and pathology.

Significance

Amyloid plaques, a key feature of Alzheimer's disease brain pathology, comprise an extracellular β-amyloid core surrounded by tissue enriched in lysosome-like organelles. As a foundation for understanding the mechanisms that drive amyloid plaque formation, we have elucidated the cellular origins and molecular composition of such organelles. The majority of the lysosomes at amyloid plaques reside within swollen neuronal axons. Interestingly, these organelles contain low levels of multiple luminal lysosomal proteases and closely resemble a lysosome subpopulation that naturally occurs in distal neuronal processes. These results suggest that extracellular β-amyloid deposits cause a local impairment in retrograde axonal transport, leading to the accumulation of lysosome precursors and a blockade in their further maturation that has implications for both β-amyloid production and clearance.

Author contributions: S.G., P.Y., J.G., P.D.C., and S.M.F. designed research; S.G., P.Y., Y.W., M.S., S.P., and S.M.F. performed research; S.G., P.Y., J.G., P.D.C., and S.M.F. analyzed data; and S.G., P.D.C., and S.M.F. wrote the paper.

Reviewers: T.B., Tufts University; and J.H., University of Texas Southwestern.

The authors declare no conflict of interest.

[1]To whom correspondence may be addressed. Email: shawn.ferguson@yale.edu or pietro.decamilli@yale.edu.

This article contains supporting information online at www.pnas.org/lookup/suppl/doi:10.1073/pnas.1510329112/-/DCSupplemental.

Results

Robust Accumulation of Lysosomal Membrane Proteins at Amyloid Plaques in Mouse Models of AD. To investigate the impact of abnormal brain APP metabolism and β-amyloid–linked AD pathology on the cell biology of the brain, we pursued a comprehensive immunofluorescent staining analysis of the brains of the 5xFAD (17) and APPswe/PS1dE9 (18) mouse models of AD that transgenically express mutant forms of human APP and presenilin 1. After analysis of the immunofluorescent staining patterns for proteins of multiple cellular organelles, our major observation, in agreement with some previous studies, was that lysosome-associated membrane protein 1 (LAMP1), a component and selective marker of late endosomes and lysosomes, showed dramatic changes in staining intensity and localization in these mouse models of AD compared with those of their littermate controls [Figs. 1 *A* and *B* and 2*A* (11, 19)]. Meanwhile, markers of other compartments—including early endosomes, plasma membrane endocytic intermediates, Golgi apparatus, mitochondria, and endoplasmic reticulum—were unchanged relative to control brains (see below; Fig. 3 and Fig. S1). This abnormal LAMP1 staining was made up of large foci distributed throughout the neocortex (Fig. 1 *A*–*C*) and was strikingly distinct from the much smaller LAMP1 puncta that correspond to individual lysosomes that are enriched within neuronal cell bodies of both the wild-type (WT) and AD mutant brains (Fig. 1*D*). To relate these LAMP1 accumulations to AD-related pathology, we performed double immunofluorescence staining for

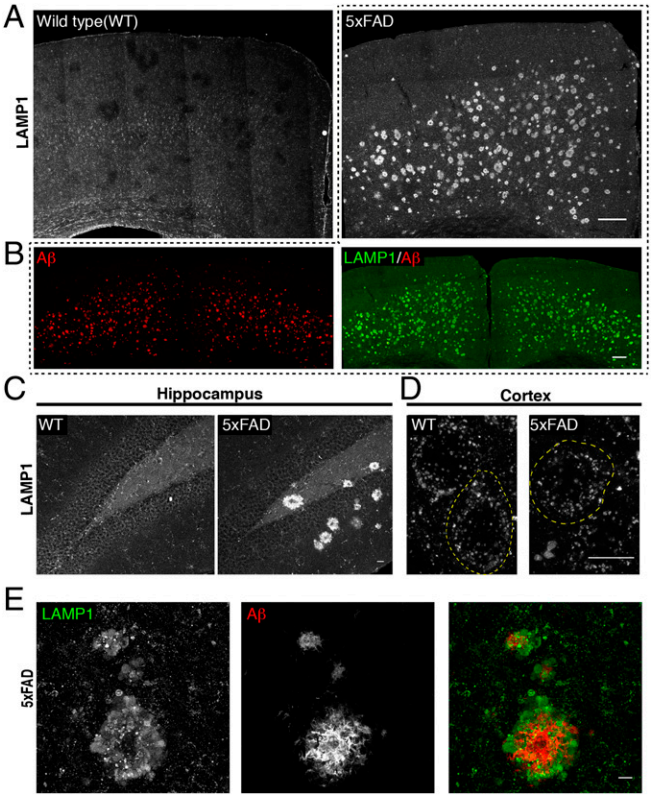

Fig. 1. LAMP1 is massively enriched at amyloid plaques. (*A*) WT and 5xFAD (6-mo-old) mouse cerebral cortex stained for LAMP1 (composites assembled from multiple images acquired with a 20× objective). (*B*) Composite image showing double labeling for LAMP1 and Aβ (expanded view of 5xFAD sample from *A*). (*C*) LAMP1 localization in WT vs. 5xFAD mouse hippocampus (dentate gyrus). (*D*) LAMP1 staining of lysosomes within both WT and 5xFAD neuronal cell bodies (dashed outline, cerebral cortex). (*E*) Higher-magnification images of plaques and surrounding LAMP1 in 5xFAD cerebral cortex. [Scale bars: 200 μm (*A* and *B*), 20 μm (*C*), and 10 μm (*D* and *E*).] See also Fig. S1.

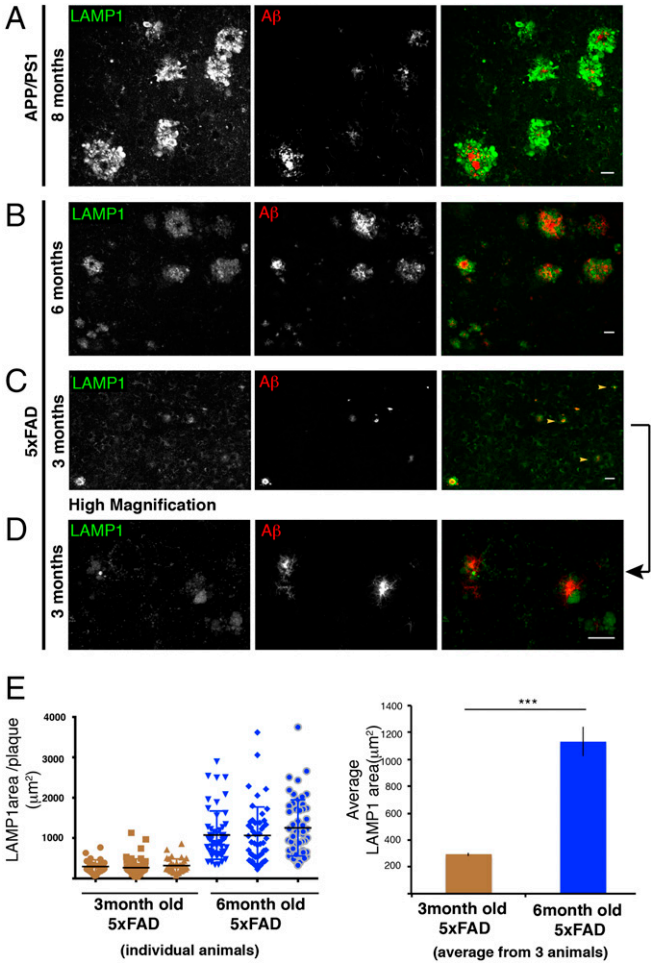

Fig. 2. LAMP1 accumulations are present at all sizes and ages of amyloid plaques. (*A*) LAMP1 and Aβ staining in 8-mo-old APP/PS1 mouse cerebral cortex. (*B* and *C*) LAMP1 and Aβ staining in cerebral cortices of 6- (*B*) and 3-mo-old 5xFAD mice (*C*). Note that the changes in LAMP1 staining intensity/area at individual plaques change in parallel with the Aβ staining. (*D*) High-magnification image of LAMP1 and Aβ staining in 3-mo-old 5xFAD mice. (*E*) Quantification of the area of lysosome accumulation around each plaque plotted as data from individual plaques and mice (*Left*) and the mean of all data (*Right*), in 3- and 6-mo-old 5xFAD mice ($n = 3$ animals per age; mean ± SD). ***$P < 0.001$ (unpaired t test). [Scale bars; 20 μm (*A*–*C*), 10 μm (*D*).]

LAMP1 and β-amyloid and found that every LAMP1 accumulation had an amyloid plaque at its core (Fig. 1 *B* and *E*). Reciprocally, every amyloid deposit that we examined was surrounded by a halo of LAMP1 immunoreactivity (>200 plaques scored per mouse; $n = 3$ mice). This close relationship between LAMP1 accumulations and β-amyloid deposits was uniformly observed in both mouse models that we studied (Fig. 2 *A* and *B*).

Lysosomes Accumulate from the Earliest Stages of Amyloid Plaque Growth. Although both amyloid plaques and LAMP1 accumulations showed considerable variability in their size and/or intensity, these two parameters were generally correlated such that larger plaques were accompanied by larger LAMP1 signals (Fig. 2*B*; see also ref. 11). Extracellular β-amyloid deposits grow over time, such that the plaques in 6-mo-old 5xFAD mice are on average larger than those in 3-mo-old mice of this strain (11). This age-dependent process of Aβ deposition was paralleled by increases in the area occupied by the LAMP1 accumulations (Fig. 2*E*). To further investigate the spatial and temporal relationship between amyloid plaques and the accumulation of LAMP1, we specifically sought

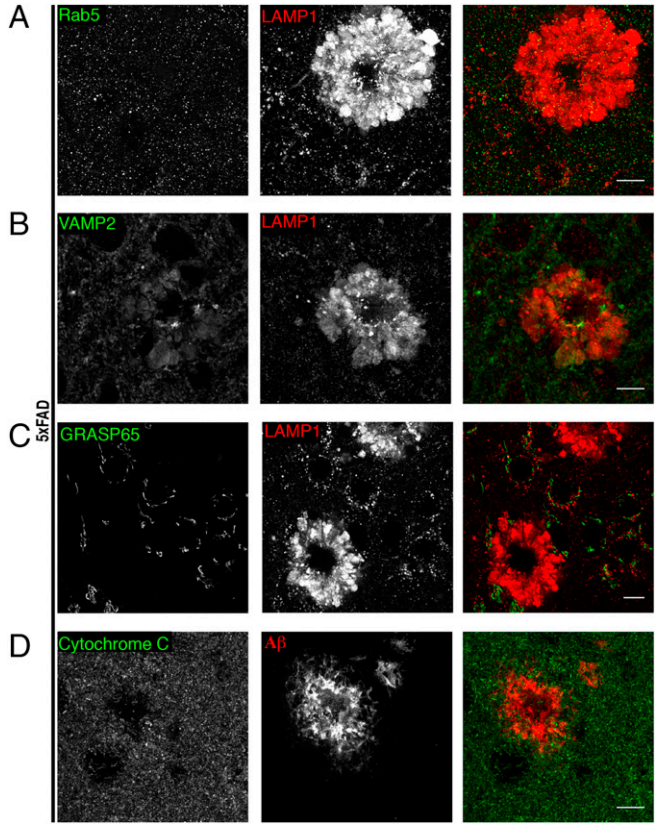

Fig. 3. Selective accumulation of LAMP1 at amyloid plaques. (*A*) Immunofluorescence staining for LAMP1 and Rab5 (early endosome marker). (*B*) Immunofluorescence staining for VAMP2 (synaptic vesicle marker) and LAMP1 costaining. (*C*) Immunofluorescence staining for GRASP65 (labels golgi) and LAMP1 double-labeling. (*D*) Mitochondria (Cytochrome C) are not enriched at amyloid plaques (Aβ labeling). (Scale bars: 10 μm.) All data in this figure were acquired from the cerebral cortices of 6-mo-old 5xFAD mice. See also Fig. S2.

out the smallest detectable amyloid deposits in young (3-mo-old) 5xFAD mice and found that even they were invariably accompanied by an adjacent LAMP1 signal (Fig. 2*C*). Likewise, LAMP1 accumulations were always found in close proximity to Aβ deposits (Fig. 2 *C* and *D*). Thus, the relationship between amyloid plaques and LAMP1 accumulation is present from the earliest detectable stages of extracellular β-amyloid deposition, and it was not possible to dissociate these two aspects of AD pathology. Thus, although the presence of LAMP1 or other lysosomal proteins around plaques has been reported previously, we demonstrate that this is not a terminal or late-stage event, but is present from the earliest stage of β-amyloid deposition.

Selectivity of Lysosome Accumulation at Amyloid Plaques. Alterations of LAMP1 localization stood out in our initial survey of organelle markers in the AD mutant mouse brains (Fig. 1 and Fig. S1). Because endosomes are important precursors in lysosome biogenesis, we further examined colocalization of LAMP1 with markers of earlier stages in the endocytic pathway. Early endosome markers (Rab5 and EEA1) were not coenriched with LAMP1 accumulations around plaques or noticeably altered throughout the neuropil (Fig. 3*A* and Fig. S1*A*). In addition, other endocytic proteins, such as Sortilin 1 or Dynamin 1, or even membrane-trafficking proteins that are genetically linked to late-onset AD (20) such as BIN1/Amphiphysin 2 and SorLA (Fig. S1 *B*–*E*), were not concentrated with LAMP1 around plaques. Representative markers of the ER (Fig. S1*F*) Golgi apparatus [GRASP65 (Fig. 3*C*)] and mitochondria [Cytochrome C (Fig. 3*D*)] were also not concentrated at amyloid plaques.

Synaptic vesicle proteins (VAMP2, vGLUT1) were variably present at such sites (Fig. 3*B* and Fig. S2*A*). However, unlike LAMP1, these proteins were not enriched at these sites compared with the surrounding neuropil, and they may reflect organelles in traffic or undigested material accumulated in LAMP1-positive organelles. Likewise, the cation-independent mannose-6-phosphate receptor—which is involved in the biosynthetic delivery of multiple lysosomal enzymes from the trans-Golgi network to endosomes/lysosomes (21) and which colocalizes with LAMP1 in neuronal cell bodies [both in WT and AD mouse brains (Fig. S2 *B* and *C*)]—was present, but was not enriched to the same extent as LAMP1 around amyloid plaques (Fig. S2*C*). Collectively, the lack of changes in markers of either the secretory or the endocytic pathway upstream of lysosomes argues against a major increase in lysosome biogenesis as an underlying cause of the lysosomal changes revealed by the LAMP1 signal.

Ultrastructural Analysis of Organelle Accumulation Surrounding Plaques. The robust LAMP1 staining surrounding amyloid plaques combined with the lack of enrichment of immunoreactive signals for markers of other organelles indicates a profound and selective overabundance of lysosomes at these sites. Accordingly, electron microscopy has revealed the presence of electron-dense organelles within swollen cellular processes that immediately surround amyloid plaques (Fig. 4*A*; refs. 9 and 14–16). Upon closer inspection at higher magnification, these electron-dense organelles have the characteristic pleomorphic morphology (electron-dense deposits and membranous material in their lumen) of lysosomes (including lysosome-autophagosome hybrids; Fig. 4 *B* and *C*). Similar structures were described in seminal electron-microscopy studies of human AD brain tissue (9). Given the central role for lysosomes as sites of macromolecule degradation, combined with roles for microglia in amyloid plaque phagocytosis and clearance (22, 23), we next investigated the contributions of microglia to these plaque-associated lysosome accumulations.

The Amyloid Plaque-Associated Lysosome Accumulation Is Largely Not of Microglial Origin. The recruitment of microglia to amyloid plaques is thought to reflect an inflammatory response that occurs in conjunction with amyloid plaque deposition in AD brains (13, 24). Because microglia and their lysosomes phagocytose and degrade Aβ, we assessed the microglial contribution to lysosome accumulations at amyloid plaques by immunostaining with an antibody against CD68, a lysosome protein exclusively expressed by cells of the monocyte/macrophage/microglia lineage (25). CD68 immunoreactivity was observed at only a subset of the small amyloid plaques in 5xFAD mice (Fig. 5*A*), with a large fraction (~60%) of small plaques not having any microglial signal associated with them at 3 mo of age (Fig. 5*B*). Even when present, CD68 staining was restricted to a much smaller area than the overall lysosome signal (Fig. 5*A*). Lysosomes were visualized in these experiments via detection of progranulin (PGRN) rather than LAMP1, an intraluminal lysosomal glycoprotein (discussed in more detail below), because both the CD68 and LAMP1 antibodies were raised in rat and thus could not be used for simultaneous labeling. Visualization of microglia via transgenic expression of GFP under control of a microglia-specific promoter [CX3CR1 (26); Fig. S3*A*] or by immunostaining for the microglial calcium-binding protein Iba1 also showed that microglial cells are only present at a subset of amyloid plaques and thus cannot account for the bulk of the plaque-associated LAMP1 signal (Fig. S3 *A* and *B*). Thus, microglia and their lysosomes do not account for the vast majority of the lysosome abundance surrounding amyloid plaques.

Plaque Proximal Lysosome Accumulations Are Predominantly Found Within Neuronal Axons. We further sought to identify the cell type and compartment where the plaque proximal lysosomes reside. Staining for glial fibrillary acidic protein (GFAP), a marker of

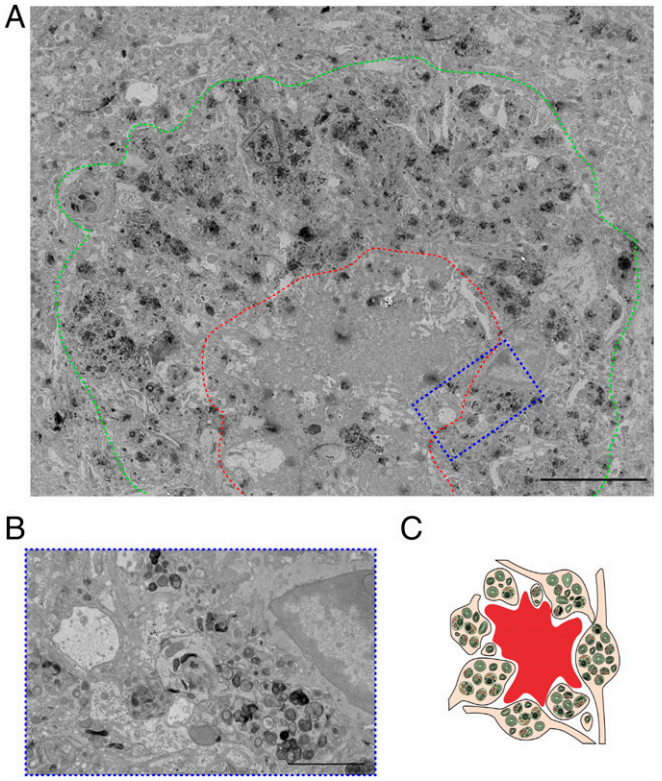

Fig. 4. Ultrastructural analysis demonstrates the intracellular accumulation of organelles with lysosome-like morphology at amyloid plaques. (*A*) Electron micrograph of APP/PS1 cerebral cortex tissue showing a central extracellular amyloid deposit (outlined in dashed red line) surrounded by electron-dense organelles (outlined with dashed green line). (Scale bar: 10 μm.) (*B*) Higher magnification of the boxed region from *A* reveals the lysosome-like morphology of organelles that accumulate within cellular processes that contact the amyloid plaque. (Scale bar: 2 μm.) (*C*) Schematic diagram depicting lysosomal accumulation within swollen cellular processes that surround an extracellular β-amyloid deposit.

astrocytes, yielded a signal that occasionally contacted sites of plaque-associated lysosome enrichment, but did not overlap with the massive LAMP1 accumulations and was not even present at many plaques (Fig. 5*C*). In addition, neuronal dendrites [as defined by microtubule-associated protein 2B (MAP2B) staining] did not overlap with sites of LAMP1 accumulation (Fig. 5*D*). However, the neurofilament (an axonal marker) staining pattern revealed that axons surrounding amyloid plaques are the sites where lysosomes are prominently enriched (Fig. 5*E*). Further supporting this conclusion, after injection of tdTomato-encoding (a red fluorescent protein) adeno-associated virus (AAV) into the hippocampal CA1 region of the 5xFAD mouse brain, tdTomato-filled axonal projections selectively demonstrated a swollen morphology at amyloid plaques and colocalized with LAMP1, whereas the dendritic projections did not (Fig. S3*C*). These results, in addition to complementary findings in the literature (10, 11, 15, 27), establish the axonal origin of the major ectopic accumulation of lysosomes at amyloid plaques.

Multiple Lysosomal Proteins Are Enriched Within Plaque-Associated Axonal Lysosomes. It is increasingly appreciated that, in addition to their degradative functions, lysosomes act as a signaling platform that integrates various metabolic inputs and initiates signals that regulate numerous downstream targets. Notably, the Rag GTPases are peripheral membrane proteins of the lysosome that communicate intracellular nutrient availability to the mTORC1 signaling pathway (28). Staining of mouse brains for RagC revealed that this important lysosome-associated signaling protein colocalized with LAMP1 on lysosomes in the cell bodies of both WT and mutant neurons (Fig. 6*A* and Fig. S4*A*). In addition, RagC was coenriched with LAMP1 in the clusters of lysosomes that surround amyloid plaques (Fig. 6*A*). Interestingly, PGRN, a protein found within the lysosome lumen, the haploinsufficiency of which causes frontotemporal dementia in humans (29, 30), also showed colocalization with LAMP1 in both neuronal cell bodies and at amyloid plaques (Fig. 6 *B* and *C* and Fig. S4 *B* and *D*). Similar robust enrichments of RagC and PGRN around plaques were also observed in the APP/PS1 mouse model (Fig. S4 *C* and *D*), confirming that this change is a general characteristic of amyloid plaques. Although microglial functions of PGRN have been recently implicated as being protective against AD pathology (31), the strong colocalization of PGRN with LAMP1 at amyloid plaques (Fig. 6*C*) compared with only partial colocalization between PGRN and CD68 (Fig. 5 *A* and *B*)] indicates that the major amyloid plaque-associated pool of PGRN resides within dystrophic axons.

Axonal Lysosome Accumulations Surrounding Amyloid Plaques Are Deficient in Their Content of Multiple Lysosomal Proteases. Having established that swollen, lysosome-filled (as assessed by their

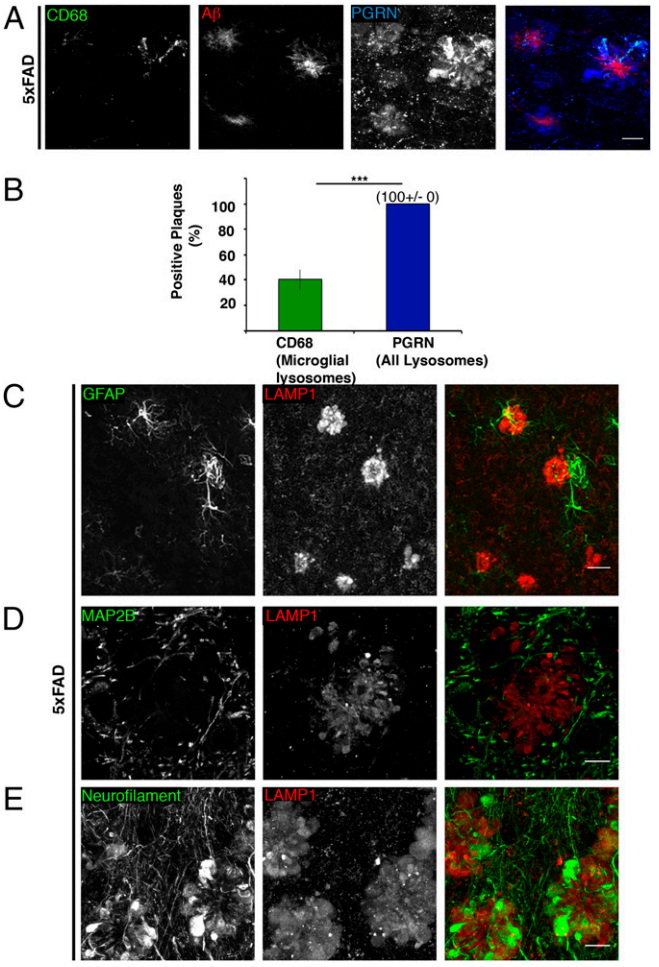

Fig. 5. Lysosome accumulations at amyloid plaques are predominantly axonal in origin. (*A*) Confocal images of cortex from 3-mo-old 5xFAD mice stained for CD68 (microglial lysosome marker), Aβ (amyloid), and PGRN (lysosomes). (*B*) Quantification of the percentage of small Aβ deposits that have either CD68 and/or PGRN associated with them [mean ± SD, $n = 3$ (3-mo-old) 5xFAD mice per experiment, >40 plaques scored per mouse]. ***$P < 0.001$. (*C*) GFAP and LAMP1 staining in 5xFAD cerebral cortex. (*D*) 5xFAD cerebral cortex mice stained for MAP2B (dendritic marker) and LAMP1. (*E*) Neurofilament and LAMP1 staining in 5xFAD cerebral cortex. (Scale bars: 10 μm.) See also Fig. S3.

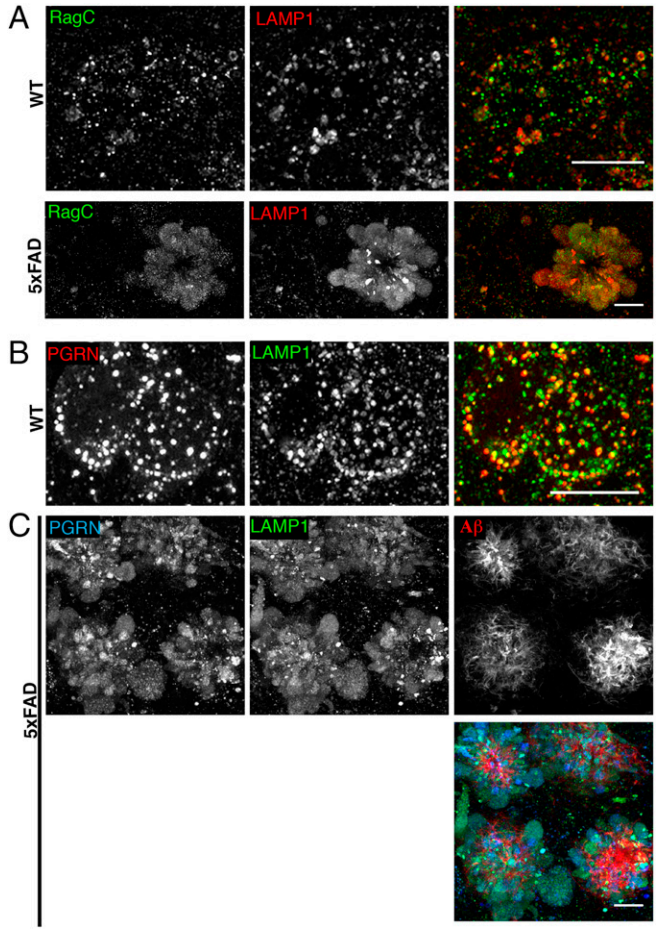

Fig. 6. RagC and PGRN are lysosome proteins that coenrich with LAMP1 at amyloid plaques. (*A*) WT and 5xFAD cerebral cortices stained for RagC and LAMP showing colocalization of the two proteins in neuronal cell bodies and around plaques. (*B*) PGRN and LAMP1 localization in WT cerebral cortex neuronal cell bodies. (*C*) Labeling for PGRN, LAMP1, and Aβ in the 6-mo-old 5xFAD cerebral cortex. (Scale bars: 10 μm.) See also Fig. S4.

LAMP1, RagC, and PGRN immunoreactivity, as well as their ultrastructural appearance) axons are a major, invariably present, feature of amyloid plaques, our attention turned to investigating their potential contributions to AD pathology. To this end, we examined in more detail the molecular identity of these lysosomes and uncovered an unexpected deficiency in their luminal protease content. Although staining for cathepsins B, D, and L yielded a signal that robustly colocalized with LAMP1-positive lysosomes in the neuronal cell bodies of both WT and AD mutant mice (Fig. 7 *A–D* and Fig. S5*A*), these lysosomal proteases were only very weakly detected within the swollen axons of amyloid plaques (Fig. 7 and Fig. S5*B*). Asparaginyl endopeptidase (AEP; also known as legumain) a lysosomal cysteine protease recently implicated in neurodegenerative disease via putative roles in the proteolysis of TDP-43 (32) and Tau (33), also failed to enrich within the axonal lysosome accumulations at amyloid plaques (Fig. 7 *D* and *E*).

Interestingly, the lack of lysosomal intraluminal protease enrichment at amyloid plaques was paralleled by their preferential presence in lysosomes of neuronal cell bodies vs. the distal neuronal compartments, even in WT brains (Fig. 8 *A* and *B*). This neuropil plus cell body staining pattern for LAMP1 vs. predominantly cell body localization for cathepsin B is quantitatively reflected by the approximately three times greater overall abundance of LAMP1 compared to cathepsin B-positive puncta in the WT cerebral cortex (2.8- ± 0.4-fold greater abundance of LAMP1 vs. cathepsin B puncta; >1,400 LAMP1 puncta examined; $n = 3$ mice). The anatomical organization of the hippocampal CA1 region is particularly well suited for the observation of organelle distribution with neuronal cell bodies vs. their axonal and dendritic projections. In this brain region, the abundance of lysosomal proteases in pyramidal neuron cell body lysosomes contrasts strongly with their near absence in the immediately adjacent stratum oriens and stratum radiatum—i.e., regions where axons and dendrites predominate over neuronal cell bodies (Fig. 8*C* and Fig. S5*D*)]. In contrast, as in the case of lysosomes observed at amyloid plaques, both RagC and PGRN were more frequently observed within the processes (Fig. S5*A* and Fig. S5*C*). The preferential enrichment of the luminal proteases within neuronal cell body lysosomes was also observed in cultured cortical neurons (Fig. 8*D* and Fig. S5*E*). These observations reveal the existence of distinct subpopulations of neuronal lysosomes that can be distinguished by

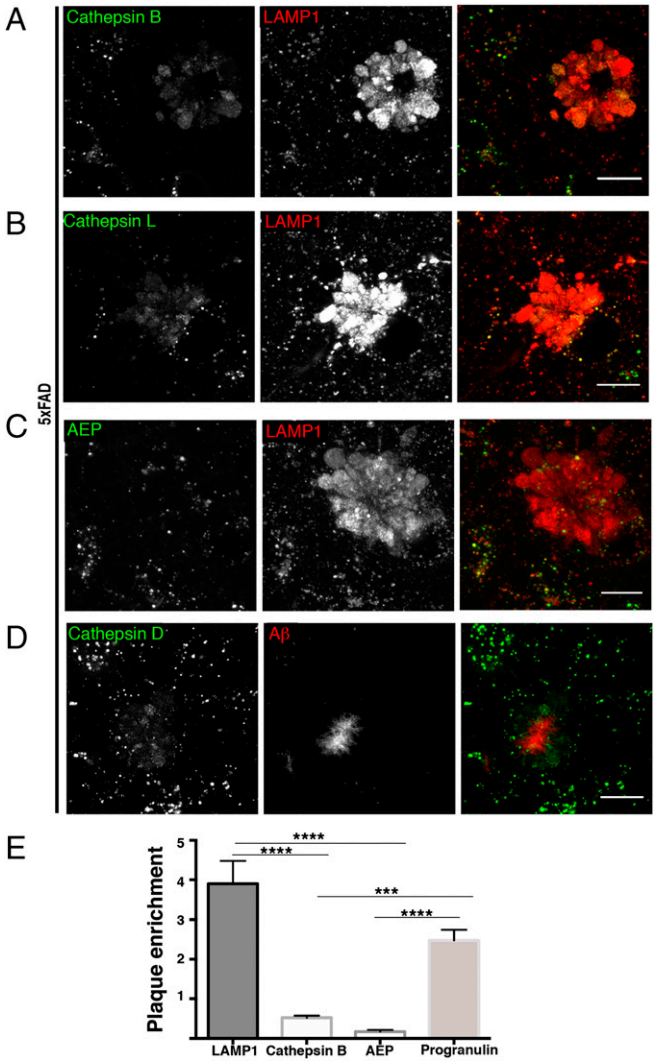

Fig. 7. Multiple lysosomal luminal proteases fail to enrich at amyloid plaques. (*A–D*) 5xFAD mouse (6 mo old) cerebral cortices double labeled for LAMP1 and either Cathepsin B (*A*) or Cathepsin L (*B*), AEP (asparaginyl endopeptidase) (*C*), or Cathespin D (*D*). (*E*) Quantification of the relative enrichment of lysosomal proteins in dystrophic axons compared with neuronal cell body lysosomes (mean ± SD). ***$P < 0.001$; ****$P < 0.0001$ (ANOVA with Dunnett's posttest; $n = 3$ experiments, five dystrophies were analyzed per condition). (Scale bars: 10 μm.)

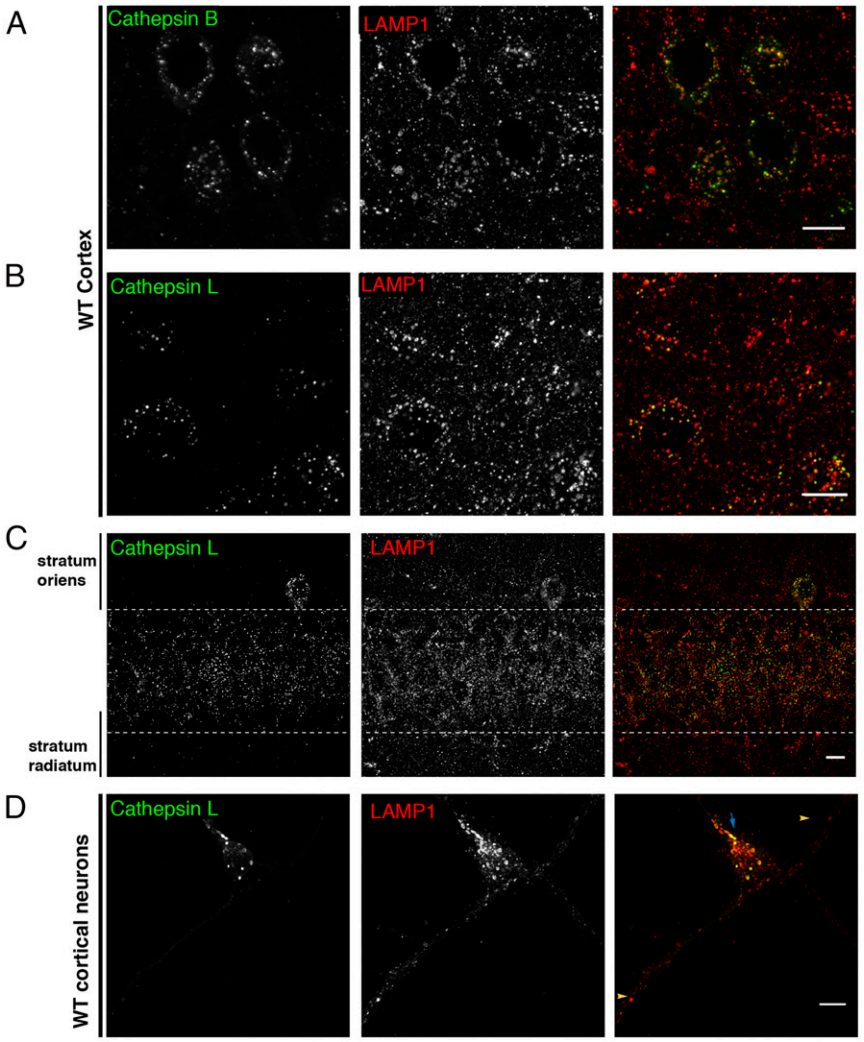

Fig. 8. Luminal proteases are preferentially enriched in the lysosomes of neuronal cell bodies. (*A* and *B*) Labeling of LAMP1 along with either Cathepsin B (*A*) or Cathepsin L (*B*) in the WT mouse cerebral cortex. (*C*) Labeling of LAMP1 along with Cathepsin B in the hippocampal CA1 region showing cathepsin L enrichment in the cell bodies compared with the stratum oriens and stratum radiatum. (*D*) Primary cortical neuron culture labeled for cathepsin L and LAMP1 showing cathepsin L enrichment in lysosomes in neuronal cell body (highlighted by blue arrow), whereas LAMP1 alone in observed in more peripheral lysosomes (yellow arrowheads). (Scale bars: 10 μm.) See also Fig. S5.

both their subcellular localization (peripheral vs. central) and their protease content. Furthermore, these patterns suggest that it is the protease-deficient, peripheral lysosome population that predominate at amyloid plaques.

β-Secretase (BACE1) Is Coenriched with Lysosomes in Dystrophic Axons. The striking abundance of lysosomes with low protease content within the axons that surround amyloid plaques raises questions about physiological consequences and potential contributions to the disease process. Interestingly, it was previously reported that β-secretase (BACE1), the protease that initiates amyloidogenic processing of APP, is present at elevated levels in human AD brains and is enriched around amyloid plaques in both mouse models of AD and in human AD brain tissue (34–37). BACE1 is a protein that traffics between the *trans*-Golgi network, plasma membrane, and endosomes before its eventual degradation in lysosomes (15, 38–40). Accordingly, BACE1 immunolabeling yielded a punctate fluorescence throughout the WT and AD mutant neuropil that did not colocalize with LAMP1-positive organelles (Fig. 9 *A* and *B*). However, in both AD models that we examined, BACE1 was enriched at plaques and colocalized extensively with LAMP1 within dystrophic axons (Fig. 9*B*). This presence of BACE1 within dystrophic axons at amyloid plaques was observed from the earliest stages of amyloid plaque formation (Fig. 9*B*). This buildup of BACE1 represents a potential consequence of unexpectedly low levels of lysosomal proteases at such sites (Fig. 7) and raises the possibility that axon dilations surrounding β-amyloid deposits may also be sites of β-amyloid production. This model is supported by reports of APP (the substrate of BACE1) localization within plaque-associated dystrophic neurites (15, 41). Because the APP C-terminal fragment that is generated by the actions of BACE1 on APP has also been shown to cause neurodegeneration due to inhibition of neurotrophin receptor retrograde axonal transport (42), BACE1 accumulation at such sites could have deleterious effects via multiple mechanisms.

Discussion

This study sheds light on AD neuropathology and also provides insight into the fundamental process of lysosome biogenesis and trafficking in neuronal axons. Our findings build on previous studies in human AD brain tissue as well as various mouse models

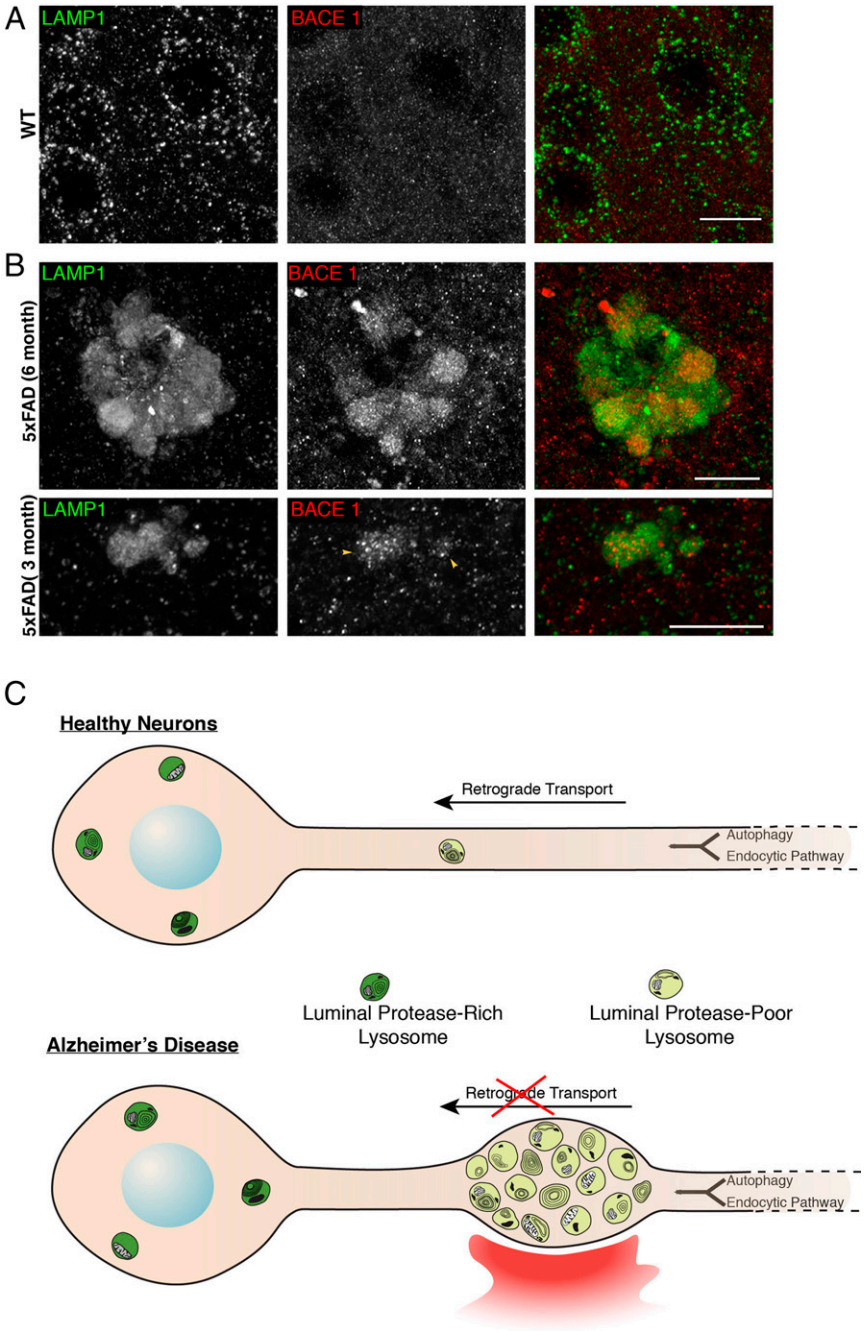

Fig. 9. BACE1 is enriched in LAMP1-positive axonal swellings at amyloid plaques. (*A*) WT cerebral cortex stained for BACE1 and LAMP1 shows their distinct patterns of localization. (*B*) 5xFAD cerebral cortex (in 3- and 6-mo-old animals) showing coaccumulation of LAMP1 and BACE1 (arrowheads, 3-mo-old sample) in dystrophic axons. (Scale bars: 10 μm.) (*C*) Schematic diagram that summarizes the distribution of lysosomes and their relative content of luminal proteases in healthy neurons as well as in AD neurons whose axons make contact with extracellular Aβ deposits.

of the disease (9–11, 14–16, 35, 43) to make the following new contributions: (*i*) We demonstrate that the lysosome accumulation at amyloid plaques is not a terminal or late-stage event but is, in fact, seen from the earliest time points of β-amyloid deposition. (*ii*) We analyzed the cellular origins of these lysosome accumulations and found that the majority of the lysosomes associated with amyloid plaques reside within neuronal axons rather than other cell types such as microglia. (*iii*) We have discovered that the axonal lysosomes that accumulate at plaques contain much lower levels of cathepsins B, D, and L (as well as AEP) than lysosomes present in neuronal cell bodies (Fig. 7 and Fig. S5*A*). (*iv*) Analysis of WT brains and cultured neurons revealed that the lower content of multiple luminal proteases is not a unique consequence of AD brain pathology, but instead reflects a general property that distinguishes lysosomes located throughout the neuropil from lysosomes residing in neuronal cell bodies. (*v*) The elevated levels of BACE1 within the swollen axons at amyloid plaques reflects a potential mechanism whereby localized defects in axonal lysosome transport and maturation could drive further amyloidogenic processing of APP.

Our analysis revealed that the lysosomes that accumulate within swollen axons of amyloid plaques most closely resemble a naturally

occurring neuronal lysosome subpopulation that preferentially resides within neuronal processes. Such organelles may represent an early stage in axonal lysosome biogenesis that arises from the fusion of lysosome precursors, including endosomes and autophagosomes, in distal regions of axons and whose further maturation requires retrograde transport to cell body proximal regions where luminal proteases can be most effectively delivered from the *trans*-Golgi network (Fig. 9*C*). This model is supported by multiple studies that point to an active process of lysosome biogenesis within axons that begins with the merging of organelles derived from the endocytic and autophagic pathways followed by further maturation toward lysosomes that is coupled to their retrograde transport (44–49). More specifically, there is a high level of constitutive autophagosome biogenesis that occurs within distal regions of axons (46, 48, 50, 51). These autophagosomes fuse with endosomes and acquire endocytic cargos and late endosome/lysosome marker proteins such as LAMP1 (46, 48, 49). These initial steps of convergence between the endocytic and autophagic pathways are accompanied by luminal acidification and coincide with a switch toward a predominantly dynein-driven transport in the retrograde direction (48, 52). Although endocytic organelles and autophagosomes fuse within distal axons and begin to mature toward a lysosomal identity, the full acquisition of degradative activity only occurs after these hybrid organelles have been successfully transported back to near the cell body region (45, 48, 51, 52). We propose that extracellular amyloid deposits trigger axonal accumulations of peripheral (immature) lysosomes through a block in their retrograde transport (Fig. 9*C*). Direct contact of the axonal plasma membrane with amyloid fibrils or oligomers could trigger such a block through calcium-mediated signals (53, 54) (Fig. 9*C*). In support of this model of amyloid-induced retrograde traffic defects, we note that the axonal lysosome-like organelles found within axons at plaques are strikingly similar to the organelles that accumulate at the distal side of sites where axon transport is acutely blocked (55).

The relatively low levels of multiple luminal proteases in dystrophic axons of amyloid plaques are contrasted by the enrichment of PGRN (also a luminal protein) at such sites (Fig. 6 and Fig. S4). These observations suggest that PGRN is delivered to lysosomes by a trafficking route that is distinct from the luminal proteases. One possibility is that at least a portion of neuronal PGRN is acquired by the endocytic uptake in axon terminals of PGRN that is secreted by either neuronal or glial cells (29). Such uptake could either occur through a sortilin-dependent mechanism (29, 56) or via the binding of PGRN to a novel plasma membrane receptor. Alternatively, PGRN could be delivered to axonal lysosome precursors by an intracellular trafficking route that is distinct from that taken by cathepsins. Addressing these questions will require a more comprehensive understanding of the PGRN trafficking itinerary in neurons. Our observations of PGRN at amyloid plaques in mouse models of AD provide new insight into the cellular and subcellular origins of amyloid-plaque–associated PGRN accumulations that have previously been reported in human AD brain tissue (57, 58). In support of a model wherein amyloid plaques trigger axonal accumulation of a naturally occurring lysosomal subpopulation, PGRN was also more prominently present than cathepsins in the peripherally located lysosomes in the WT brain (Figs. S4*B* and S5*C*).

PGRN is of particular interest in the context of neurodegenerative disease because its haploinsufficiency causes frontotemporal dementia in humans (59, 60), and putative roles for PGRN in AD have been proposed (61). Interestingly, it was recently reported (based on genetic perturbations) that microglial PGRN limits amyloid plaque deposition in a mouse AD model (31). However, although microglia can phagocytose and digest aggregated Aβ in a lysosome-dependent manner (22, 62, 63), our data indicate that they contributed only a small part to the steady-state pool of PGRN and lysosomes around amyloid plaques. Our results do not rule out physiologically important roles for microglia and their lysosomes in β-amyloid metabolism, as proposed by recent studies (64–66). However, we establish that the majority of the PGRN that accumulates at amyloid plaques is axonal.

Although elevated total BACE 1 protein levels and their accumulation at amyloid plaques is an established component of human AD brain pathology (34–37), the underlying mechanisms have remained unclear. Because BACE1 is normally abundantly localized to axons (34) and is degraded by lysosomes (15, 38, 39), our observations suggest that cathepsin levels might be rate-limiting for the efficient degradation of BACE1 and thus lead to its high abundance at such sites. This concept is supported by previous studies that detected reductions in amyloid plaque burden after the enhancement of cathepsin activity in mouse models of AD (67–69). Although such studies largely focused on cathepsin-mediated Aβ peptide degradation as a mechanism for explaining the overall reduction in Aβ levels and amyloid plaque load, the possibility that elevated cathepsin levels/activity exerted additional antiamyloidogenic effects via enhanced BACE1 breakdown requires further investigation in light of our new findings.

This study, in conjunction with corroborating findings in human postmortem AD tissue (9–11, 14–16, 34–37, 43), suggests that a disruption in the retrograde transport and maturation of axonal lysosomes represents one of the earliest aspects of amyloid plaque biogenesis and raises new questions about both the signals and membrane-trafficking mechanisms that underlie this phenotype, as well as its impact on AD pathogenesis. This model wherein axonal accumulations of immature lysosomes at amyloid plaques act as pathologically meaningful sites of Aβ synthesis is consistent with lesion studies that support an axonal origin of Aβ (70, 71), as well as with evidence for the endolysosomal localization and APP processing activities of γ-secretase (72–75). The further elucidation of mechanisms whereby extracellular Aβ deposits negatively affect the axonal transport and maturation of lysosomes could lead to new therapeutic opportunities for limiting the amyloidogenic processing of APP.

Experimental Procedures

Mouse Strains. Animal procedures were approved by and carried out in accordance with guidelines established by the Institutional Animal Care and Use Committee at Yale University. The 5xFAD (17) and APPswe/PS1dE9 (18) mice have been described. Heterozygous male transgenic mice were bred with C57BL/6J females, and the progeny were genotyped by PCR. WT littermates served as controls for experiments involving transgenic mice. For microglia visualization, mice with the CX(3)CR1 gene replaced by GFP [The Jackson Laboratory (26)] were mated with the 5xFAD mice.

Transcardial Perfusion. PBS and 4% (wt/vol) paraformaldehyde were sequentially administered to anesthetized mice (Ketamine/Xylazine) by transcardiac perfusion. The brain was then collected and postfixed overnight at 4 °C.

Immunofluorescence Staining of Brain Sections. After fixation and washes, coronal brain sections were cut (30 μm thick) with a vibratome (Leica, VT1000S) and stored in PBS–azide at 4 °C. Samples were blocked (0.2% Triton–PBS–3% BSA) for 5 h at room temperature, followed by incubation with primary antibody (diluted in blocking buffer), overnight at 4 °C. Sections were washed in 0.2% PBS–BSA (3 × 10 min) and then labeled with fluorescently labeled secondary antibodies diluted in blocking buffer for 4 h at room temperature. Sections were washed again for 30 min and then mounted on glass slides with Prolong GOLD mounting medium (Life Technologies).

Antibodies and Reagents. Antibody information (including commercial sources and dilutions) can be found in Table S1. Additional tissue-staining reagents included Thioflavin S (Sigma-Aldrich) and BODIPY-FL-Pepstatin A (Life Technologies).

Microscopy. The 16-bit images (512 × 512 pixels) were acquired with a laser-scanning confocal microscope (LSM 710; Carl Zeiss) equipped with a 63× plano Apo (NA 1.4) oil-immersion objective lens or a 20× (NA 0.8) objective and a QUASAR (Quiet Spectral array) photomultiplier tube detector. Z-stacks with a step size of 0.49 and 1.0 μm were routinely acquired with the 63× and 20× objectives, respectively. Spinning disk confocal images were obtained by using the UltraVIEW VoX system (PerkinElmer), including an inverted

microscope [Nikon Ti-E Eclipse equipped with a spinning disk confocal scan head (CSU-X1; Yokogawa)] driven by Volocity (PerkinElmer) software. Images were acquired without binning with a 14-bit (1,000 × 1,000) EM CCD (Hamamatsu Photonics). Images were obtained by using a 40× oil-immersion objective (1.3 NA) and a 20× objective (0.75 NA). Z-stacks with a step size of 0.3 μm were acquired by using the 40× objective.

Quantification of Axonal Lysosome Accumulation at Plaques. Coronal brain sections from FAD (3- or 6-mo-old) mice were costained for LAMP1 and Aβ and imaged by spinning disk microscopy. Images (Z-stack images that encompassed LAMP1 and Aβ signals, typically 35–50 planes with 0.3-μm step size) of amyloid plaques and the LAMP1 accumulations around them were acquired (40× objective) from the cerebral cortex. Images were subsequently processed by using ImageJ software. Maximum intensity projections of the LAMP1 and amyloid staining were made, regions of interest were manually outlined, and the area associated with the outlined region was calculated by using ImageJ.

Quantification Amyloid Plaques Association with Microglial Lysosomes. Coronal sections from 3-mo-old 5xFAD mice were stained with antibodies to Aβ (amyloid deposits), CD68 (microglial lysosomes), and PGRN (all lysosomes) and imaged by laser-scanning confocal microscopy using a 20× objective (NA 1.4). Images of the three channels were overlaid, and all plaques with in-focus Aβ and a diameter of <32 μm (this cut-off ensured analysis of discrete plaques) were examined for association with the two lysosome makers. All plaques with any overlap of CD68 signal with either Aβ or PGRN were scored as CD68-positive.

Measurement of Lysosome Protein Enrichment at Amyloid Plaques. Brain sections from 6-mo-old 5xFAD mice were costained for LAMP1 and either cathepsin B, PGRN, or AEP and imaged by laser-scanning confocal microscopy (63× objective). Z-stacks were acquired to encompass a selected amyloid plaque (typically 12–15 Z-planes with a step size of 0.49 μm). ImageJ software was used to calculate the enrichment of the respective lysosomal proteins in the dystrophies. To this end, regions of interest (10 per mouse) were outlined within amyloid plaque axonal dystrophies and over cell body lysosomes within the same image. The mean intensity in each such region was determined, and the ratio between them was calculated for each lysosomal protein. At least three different 5xFAD mice were analyzed for each condition.

Electron Microscopy. Mice were perfused with 2.5% paraformaldehyde and 2% glutaraldehyde in 0.1 M cacodylate buffer (pH 7.4), postfixed in 1% OsO4 and 1% K4Fe(CN)6, and en bloc stained in 2% aqueous uranyl acetate before dehydration and embedding in Epon. Ultrathin sections (60–70 nm) were contrasted with 2% uranyl acetate and lead citrate and observed in a Philips CM10 microscope at 80 kV. Images were acquired with a Morada 1 k × 1 k CCD camera (Olympus).

Recombinant AAV Production and Injection. A sequence comprising the Lck membrane targeting sequence fused to the tdTomato red fluorescent protein was ligated between the inverted terminal repeat sites of an AAV2 packaging plasmid that included a CAG promoter and WPRE/SV40 sequences. HEK293T cells were cotransfected with this construct and a helper plasmid pDP2 (76) and harvested 96 h later. Viruses were purified via iodixanol density centrifugation (77) and titrated by transducing HEK293T cells. AAV2–Lck–tdTomato virus was injected stereotactically into 4-mo-old 5xFAD mice. Mice were anesthetized with i.p. injection of Ketamine–Xylazine. A thin glass pipette filled with virus solution (titer ~1×10^{12} virion per liter) was placed in the following coordinates: anterior–posterior, −2.1 mm from Bregma; medial–lateral, 1.5 mm from midline; and dorsal–ventral, −1.3 mm from the surface of thinned skull. Then, 0.5 μL of virus solution was injected, and the pipette was removed 15 min after injection. Brains were harvested and analyzed 2–4 wk after injection.

Neuron Culture Primary cultures of mouse cortical neurons were prepared and stained for immunofluorescence analysis as described (78).

Statistical Methods. Data are represented as mean ± SD unless specified otherwise. Data are representative of experimental results that were obtained from at least three experiments (animals of each genotype and/or age). Data were analyzed by using PRISM software using the indicated statistical tests.

ACKNOWLEDGMENTS. We thank Frank Wilson and Agnes Roczniak-Ferguson for superb management and maintenance of lab infrastructure; Wendolyn Hill for assistance with illustrations; and Louise Lucast and Lijuan Liu for outstanding technical assistance with mouse colony management. This work was supported in part by NIH Grants GM105718 (to S.M.F.), NS36251, DK45735, and DA018343 (to P.D.C.), and HL06815 (to J.G.). Both S.M.F. and P.D.C. were supported by the Ellison Medical Foundation. S.M.F. was also supported by the Consortium for Frontotemporal Dementia Research. Microscopy studies were supported by the Yale University Program in Cellular Neuroscience, Neurodegeneration and Repair imaging facility.

1. Selkoe DJ (2013) SnapShot: Pathobiology of Alzheimer's disease. Cell 154(2):468–468.e1.
2. Karran E, Mercken M, De Strooper B (2011) The amyloid cascade hypothesis for Alzheimer's disease: An appraisal for the development of therapeutics. *Nat Rev Drug Discov* 10(9):698–712.
3. Tanzi RE, Bertram L (2005) Twenty years of the Alzheimer's disease amyloid hypothesis: a genetic perspective. *Cell* 120(4):545–555.
4. Holtzman DM, Morris JC, Goate AM (2011) Alzheimer's disease: The challenge of the second century. *Sci Transl Med* 3(77):sr1.
5. Jonsson T, et al. (2012) A mutation in APP protects against Alzheimer's disease and age-related cognitive decline. *Nature* 488(7409):96–99.
6. LaFerla FM, Green KN (2012) Animal models of Alzheimer disease. Cold Spring Harbor Perspect Med 2(11):a006320.
7. Nixon RA (2007) Autophagy, amyloidogenesis and Alzheimer disease. *J Cell Sci* 120(Pt 23): 4081–4091.
8. Serrano-Pozo A, Frosch MP, Masliah E, Hyman BT (2011) Neuropathological alterations in Alzheimer disease. Cold Spring Harbor Perspect Med 1(1):a006189.
9. Terry RD, Gonatas NK, Weiss M (1964) Ultrastructural studies in Alzheimer's presenile dementia. *Am J Pathol* 44(2):269–297.
10. Fiala JC (2007) Mechanisms of amyloid plaque pathogenesis. *Acta Neuropathol* 114(6):551–571.
11. Condello C, Schain A, Grutzendler J (2011) Multicolor time-stamp reveals the dynamics and toxicity of amyloid deposition. Sci Rep 1:19.
12. Tsai J, Grutzendler J, Duff K, Gan WB (2004) Fibrillar amyloid deposition leads to local synaptic abnormalities and breakage of neuronal branches. *Nat Neurosci* 7(11): 1181–1183.
13. Itagaki S, McGeer PL, Akiyama H, Zhu S, Selkoe D (1989) Relationship of microglia and astrocytes to amyloid deposits of Alzheimer disease. *J Neuroimmunol* 24(3):173–182.
14. Cataldo AM, Paskevich PA, Kominami E, Nixon RA (1991) Lysosomal hydrolases of different classes are abnormally distributed in brains of patients with Alzheimer disease. *Proc Natl Acad Sci USA* 88(24):10998–11002.
15. Kandalepas PC, et al. (2013) The Alzheimer's β-secretase BACE1 localizes to normal presynaptic terminals and to dystrophic presynaptic terminals surrounding amyloid plaques. *Acta Neuropathol* 126(3):329–352.
16. Nixon RA, et al. (2005) Extensive involvement of autophagy in Alzheimer disease: An immuno-electron microscopy study. *J Neuropathol Exp Neurol* 64(2):113–122.
17. Oakley H, et al. (2006) Intraneuronal beta-amyloid aggregates, neurodegeneration, and neuron loss in transgenic mice with five familial Alzheimer's disease mutations: potential factors in amyloid plaque formation. J Neurosci 26(40):10129–10140.
18. Garcia-Alloza M, et al. (2006) Characterization of amyloid deposition in the APPswe/PS1dE9 mouse model of Alzheimer disease. *Neurobiol Dis* 24(3):516–524.
19. Barrachina M, Maes T, Buesa C, Ferrer I (2006) Lysosome-associated membrane protein 1 (LAMP-1) in Alzheimer's disease. *Neuropathol Appl Neurobiol* 32(5):505–516.
20. Lambert JC, et al.; European Alzheimer's Disease Initiative (EADI); Genetic and Environmental Risk in Alzheimer's Disease; Alzheimer's Disease Genetic Consortium; Cohorts for Heart and Aging Research in Genomic Epidemiology (2013) Meta-analysis of 74,046 individuals identifies 11 new susceptibility loci for Alzheimer's disease. *Nat Genet* 45(12):1452–1458.
21. Braulke T, Bonifacino JS (2009) Sorting of lysosomal proteins. *Biochim Biophys Acta* 1793(4):605–614.
22. Majumdar A, et al. (2007) Activation of microglia acidifies lysosomes and leads to degradation of Alzheimer amyloid fibrils. *Mol Biol Cell* 18(4):1490–1496.
23. Wyss-Coray T, et al. (2001) TGF-beta1 promotes microglial amyloid-beta clearance and reduces plaque burden in transgenic mice. *Nat Med* 7(5):612–618.
24. Wyss-Coray T (2006) Inflammation in Alzheimer disease: Driving force, bystander or beneficial response? *Nat Med* 12(9):1005–1015.
25. Ulvestad E, Williams K, Mørk S, Antel J, Nyland H (1994) Phenotypic differences between human monocytes/macrophages and microglial cells studied in situ and in vitro. *J Neuropathol Exp Neurol* 53(5):492–501.
26. Jung S, et al. (2000) Analysis of fractalkine receptor CX(3)CR1 function by targeted deletion and green fluorescent protein reporter gene insertion. *Mol Cell Biol* 20(11): 4106–4114.
27. Adalbert R, et al. (2009) Severely dystrophic axons at amyloid plaques remain continuous and connected to viable cell bodies. Brain 132(Pt 2):402–416.
28. Efeyan A, Comb WC, Sabatini DM (2015) Nutrient-sensing mechanisms and pathways. *Nature* 517(7534):302–310.
29. Hu F, et al. (2010) Sortilin-mediated endocytosis determines levels of the frontotemporal dementia protein, progranulin. *Neuron* 68(4):654–667.
30. Cenik B, Sephton CF, Kutluk Cenik B, Herz J, Yu G (2012) Progranulin: A proteolytically processed protein at the crossroads of inflammation and neurodegeneration. *J Biol Chem* 287(39):32298–32306.

31. Minami SS, et al. (2014) Progranulin protects against amyloid β deposition and toxicity in Alzheimer's disease mouse models. *Nat Med* 20(10):1157–1164.
32. Herskowitz JH, et al. (2012) Asparaginyl endopeptidase cleaves TDP-43 in brain. *Proteomics* 12(15-16):2455–2463.
33. Zhang Z, et al. (2014) Cleavage of tau by asparagine endopeptidase mediates the neurofibrillary pathology in Alzheimer's disease. *Nat Med* 20(11):1254–1262.
34. Zhao J, et al. (2007) Beta-site amyloid precursor protein cleaving enzyme 1 levels become elevated in neurons around amyloid plaques: Implications for Alzheimer's disease pathogenesis. *J Neurosci* 27(14):3639–3649.
35. Zhang XM, et al. (2009) Beta-secretase-1 elevation in transgenic mouse models of Alzheimer's disease is associated with synaptic/axonal pathology and amyloidogenesis: Implications for neuritic plaque development. *Eur J Neurosci* 30(12): 2271–2283.
36. Fukumoto H, Cheung BS, Hyman BT, Irizarry MC (2002) Beta-secretase protein and activity are increased in the neocortex in Alzheimer disease. *Arch Neurol* 59(9): 1381–1389.
37. Holsinger RM, McLean CA, Beyreuther K, Masters CL, Evin G (2002) Increased expression of the amyloid precursor beta-secretase in Alzheimer's disease. *Ann Neurol* 51(6):783–786.
38. Koh YH, von Arnim CA, Hyman BT, Tanzi RE, Tesco G (2005) BACE is degraded via the lysosomal pathway. *J Biol Chem* 280(37):32499–32504.
39. Ye X, Cai Q (2014) Snapin-mediated BACE1 retrograde transport is essential for its degradation in lysosomes and regulation of APP processing in neurons. *Cell Reports* 6(1):24–31.
40. Prabhu Y, et al. (2012) Adaptor protein 2-mediated endocytosis of the β-secretase BACE1 is dispensable for amyloid precursor protein processing. *Mol Biol Cell* 23(12): 2339–2351.
41. Cras P, et al. (1991) Senile plaque neurites in Alzheimer disease accumulate amyloid precursor protein. *Proc Natl Acad Sci USA* 88(17):7552–7556.
42. Salehi A, et al. (2006) Increased App expression in a mouse model of Down's syndrome disrupts NGF transport and causes cholinergic neuron degeneration. *Neuron* 51(1):29–42.
43. Cataldo AM, Nixon RA (1990) Enzymatically active lysosomal proteases are associated with amyloid deposits in Alzheimer brain. *Proc Natl Acad Sci USA* 87(10):3861–3865.
44. Maday S, Twelvetrees AE, Moughamian AJ, Holzbaur EL (2014) Axonal transport: Cargo-specific mechanisms of motility and regulation. *Neuron* 84(2):292–309.
45. Overly CC, Hollenbeck PJ (1996) Dynamic organization of endocytic pathways in axons of cultured sympathetic neurons. *J Neurosci* 16(19):6056–6064.
46. Hollenbeck PJ (1993) Products of endocytosis and autophagy are retrieved from axons by regulated retrograde organelle transport. *J Cell Biol* 121(2):305–315.
47. Lee S, Sato Y, Nixon RA (2011) Lysosomal proteolysis inhibition selectively disrupts axonal transport of degradative organelles and causes an Alzheimer's-like axonal dystrophy. *J Neurosci* 31(21):7817–7830.
48. Maday S, Wallace KE, Holzbaur EL (2012) Autophagosomes initiate distally and mature during transport toward the cell soma in primary neurons. *J Cell Biol* 196(4): 407–417.
49. Cheng XT, Zhou B, Lin MY, Cai Q, Sheng ZH (2015) Axonal autophagosomes recruit dynein for retrograde transport through fusion with late endosomes. *J Cell Biol* 209(3):377–386.
50. Lee S, Sato Y, Nixon RA (2011) Primary lysosomal dysfunction causes cargo-specific deficits of axonal transport leading to Alzheimer-like neuritic dystrophy. *Autophagy* 7(12):1562–1563.
51. Boland B, et al. (2008) Autophagy induction and autophagosome clearance in neurons: Relationship to autophagic pathology in Alzheimer's disease. *J Neurosci* 28(27): 6926–6937.
52. Fu MM, Nirschl JJ, Holzbaur EL (2014) LC3 binding to the scaffolding protein JIP1 regulates processive dynein-driven transport of autophagosomes. *Dev Cell* 29(5): 577–590.
53. Wu HY, et al. (2010) Amyloid beta induces the morphological neurodegenerative triad of spine loss, dendritic simplification, and neuritic dystrophies through calcineurin activation. *J Neurosci* 30(7):2636–2649.
54. Shah SB, et al. (2009) Examination of potential mechanisms of amyloid-induced defects in neuronal transport. *Neurobiol Dis* 36(1):11–25.
55. Tsukita S, Ishikawa H (1980) The movement of membranous organelles in axons. Electron microscopic identification of anterogradely and retrogradely transported organelles. *J Cell Biol* 84(3):513–530.
56. Carrasquillo MM, et al. (2010) Genome-wide screen identifies rs646776 near sortilin as a regulator of progranulin levels in human plasma. *Am J Hum Genet* 87(6):890–897.
57. Gliebus G, Rosso A, Lippa CF (2009) Progranulin and beta-amyloid distribution: A case report of the brain from preclinical PS-1 mutation carrier. *Am J Alzheimers Dis Other Demen* 24(6):456–460.
58. Pereson S, et al. (2009) Progranulin expression correlates with dense-core amyloid plaque burden in Alzheimer disease mouse models. *J Pathol* 219(2):173–181.
59. Baker M, et al. (2006) Mutations in progranulin cause tau-negative frontotemporal dementia linked to chromosome 17. *Nature* 442(7105):916–919.
60. Cruts M, et al. (2006) Null mutations in progranulin cause ubiquitin-positive frontotemporal dementia linked to chromosome 17q21. *Nature* 442(7105):920–924.
61. Perry DC, et al. (2013) Progranulin mutations as risk factors for Alzheimer disease. *JAMA Neurol* 70(6):774–778.
62. Koenigsknecht J, Landreth G (2004) Microglial phagocytosis of fibrillar beta-amyloid through a beta1 integrin-dependent mechanism. *J Neurosci* 24(44):9838–9846.
63. Paresce DM, Ghosh RN, Maxfield FR (1996) Microglial cells internalize aggregates of the Alzheimer's disease amyloid beta-protein via a scavenger receptor. *Neuron* 17(3): 553–565.
64. Guillot-Sestier MV, et al. (2015) Il10 deficiency rebalances innate immunity to mitigate Alzheimer-like pathology. *Neuron* 85(3):534–548.
65. Chakrabarty P, et al. (2015) IL-10 alters immunoproteostasis in APP mice, increasing plaque burden and worsening cognitive behavior. *Neuron* 85(3):519–533.
66. Condello C, Yuan P, Schain A, Grutzendler J (2015) Microglia constitute a barrier that prevents neurotoxic protofibrillar Aβ42 hotspots around plaques. *Nat Commun* 6: 6176.
67. Wang C, Sun B, Zhou Y, Grubb A, Gan L (2012) Cathepsin B degrades amyloid-β in mice expressing wild-type human amyloid precursor protein. *J Biol Chem* 287(47): 39834–39841.
68. Mueller-Steiner S, et al. (2006) Antiamyloidogenic and neuroprotective functions of cathepsin B: Implications for Alzheimer's disease. *Neuron* 51(6):703–714.
69. Yang DS, et al. (2011) Reversal of autophagy dysfunction in the TgCRND8 mouse model of Alzheimer's disease ameliorates amyloid pathologies and memory deficits. Brain 134(Pt 1):258–277.
70. Sheng JG, Price DL, Koliatsos VE (2002) Disruption of corticocortical connections ameliorates amyloid burden in terminal fields in a transgenic model of Abeta amyloidosis. *J Neurosci* 22(22):9794–9799.
71. Lazarov O, Lee M, Peterson DA, Sisodia SS (2002) Evidence that synaptically released beta-amyloid accumulates as extracellular deposits in the hippocampus of transgenic mice. *J Neurosci* 22(22):9785–9793.
72. Yu WH, et al. (2004) Autophagic vacuoles are enriched in amyloid precursor protein-secretase activities: Implications for beta-amyloid peptide over-production and localization in Alzheimer's disease. *Int J Biochem Cell Biol* 36(12):2531–2540.
73. Pasternak SH, et al. (2003) Presenilin-1, nicastrin, amyloid precursor protein, and gamma-secretase activity are co-localized in the lysosomal membrane. *J Biol Chem* 278(29):26687–26694.
74. Runz H, et al. (2002) Inhibition of intracellular cholesterol transport alters presenilin localization and amyloid precursor protein processing in neuronal cells. *J Neurosci* 22(5):1679–1689.
75. Coen K, et al. (2012) Lysosomal calcium homeostasis defects, not proton pump defects, cause endo-lysosomal dysfunction in PSEN-deficient cells. *J Cell Biol* 198(1): 23–35.
76. Grimm D, Kay MA, Kleinschmidt JA (2003) Helper virus-free, optically controllable, and two-plasmid-based production of adeno-associated virus vectors of serotypes 1 to 6. Mol Ther 7(6):839–850.
77. Zolotukhin S, et al. (1999) Recombinant adeno-associated virus purification using novel methods improves infectious titer and yield. *Gene Ther* 6(6):973–985.
78. Ferguson SM, et al. (2007) A selective activity-dependent requirement for dynamin 1 in synaptic vesicle endocytosis. *Science* 316(5824):570–574.